Supplementary Information (SI) for Journal of Materials Chemistry A.
This journal is © The Royal Society of Chemistry 2026

Supplementary information

Tensile-strained silver assembly enables ampere-level electrochemical CO_2-to-CO conversion across a wide pH range

Weibo Hu,[*a] Lihua Zhu,[b] Chuyi Zhao,[b] Shuran Yao,[b] Junsong Song,[a] Jiale Chen,[a] Xiaopeng Li[*b] and Jianming Li[*a]

[a]School of New Energy, Ningbo University of Technology, Ningbo 315336, China

E-mail: huwb@nbut.edu.cn; jmli@nbut.edu.cn

[b]State Key Laboratory of Advanced Fiber Materials, College of Materials Science and Engineering, Donghua University, Shanghai 201620, China

E-mail: xiaopeng.li@dhu.edu.cn

1. Density functional theory (DFT) calculations

DFT calculations employed the Vienna Ab initio Simulation Package (VASP) with the generalized gradient approximation and Perdew-Burke-Ernzerhof (GGA-PBE) functional and PAW pseudopotentials. A 450 eV plane-wave cutoff and DFT-D3 van der Waals correction were applied. Geometries were optimized until forces < 0.05 eV/Å. A 2×2×1 *k*-mesh sampled the 4-layer Ag(111) slab, with 2% tensile strain applied to simulate grain boundary stress. Bottom-layer atoms were fixed, and edge atoms were constrained to maintain stress.

Reaction step free energies (ΔG) for CO_2RR and HER were calculated using the CHE model. Potential-dependent ΔG was calculated as ΔG (U) = ΔG (0V) - *ne*U. Gibbs free energy followed: $\Delta G = \Delta E + \Delta E_{ZPE} - T\Delta S$, where ΔE, ΔE_{ZPE}, and ΔS denote DFT energy, zero-point energy, and entropy changes at 298.15 K, respectively.

2. Electrochemical Measurements

The long-term stability test was conducted in 0.3 M K_2SO_4 (pH ≈ 3) to alleviate the salting-out effect. The lower electrolyte concentration yields a higher solution resistance, leading to obvious potential deviation under the same 0.8 × iR_s compensation ratio compared with the performance tests performed in 0.5 M K_2SO_4.

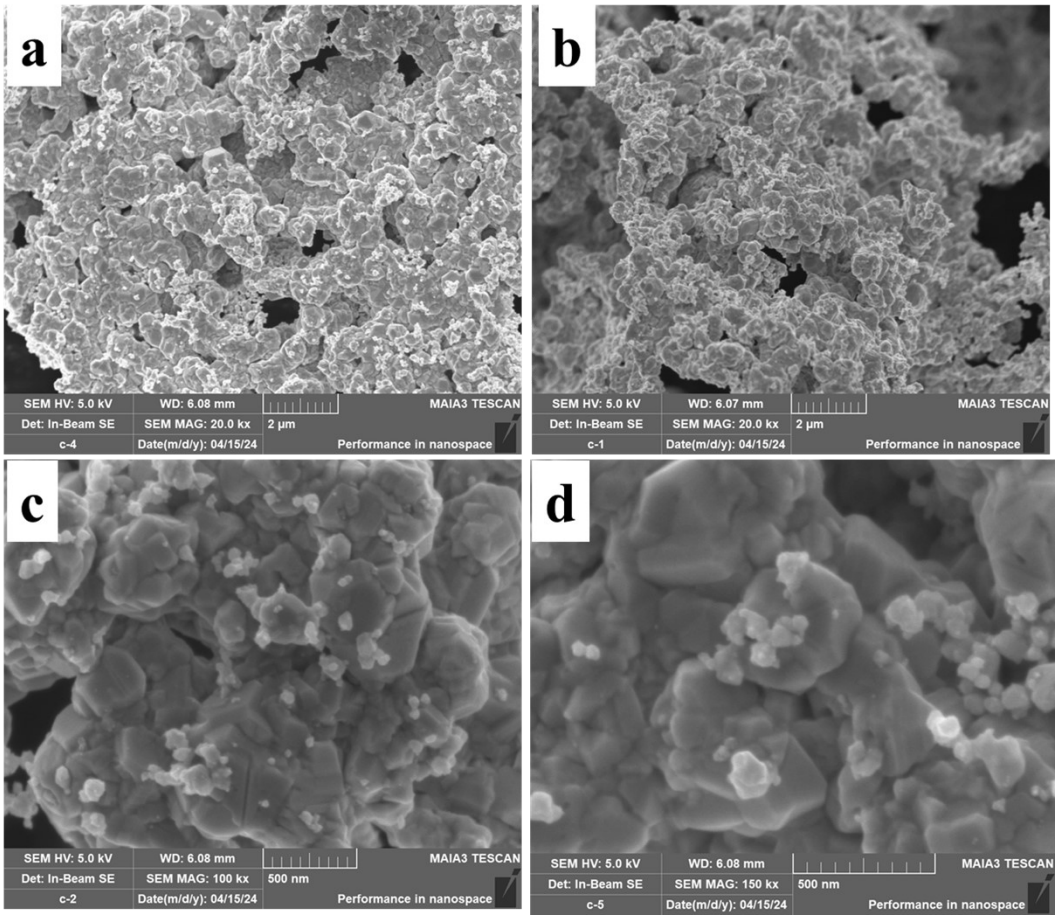

Fig. S1 SEM images of the silver sample prepared using D-glucose as the reducing agent

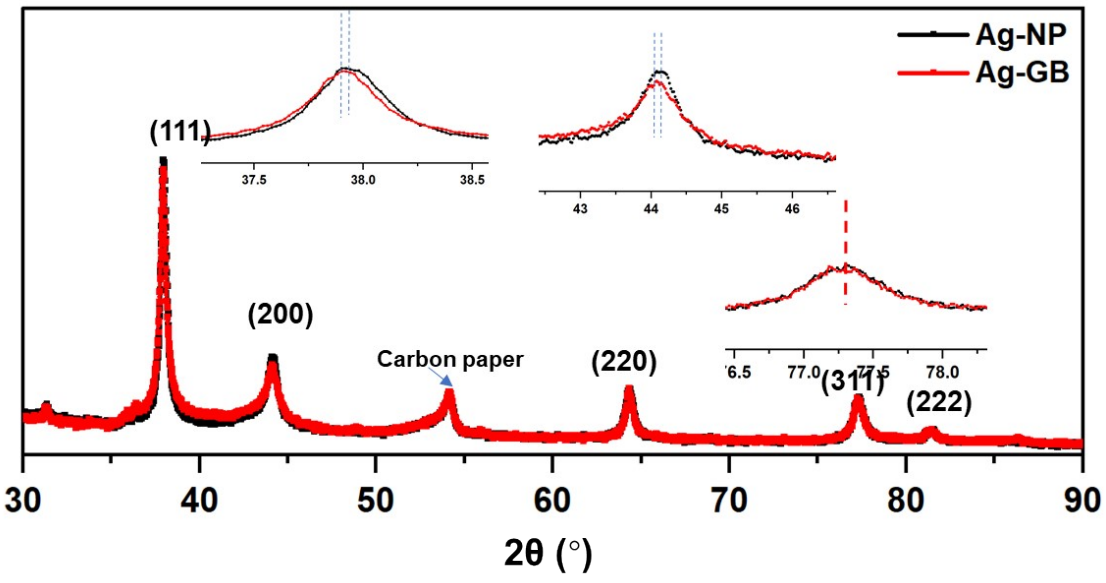

Fig. S2 XRD patterns of Ag-GB and Ag-NP.

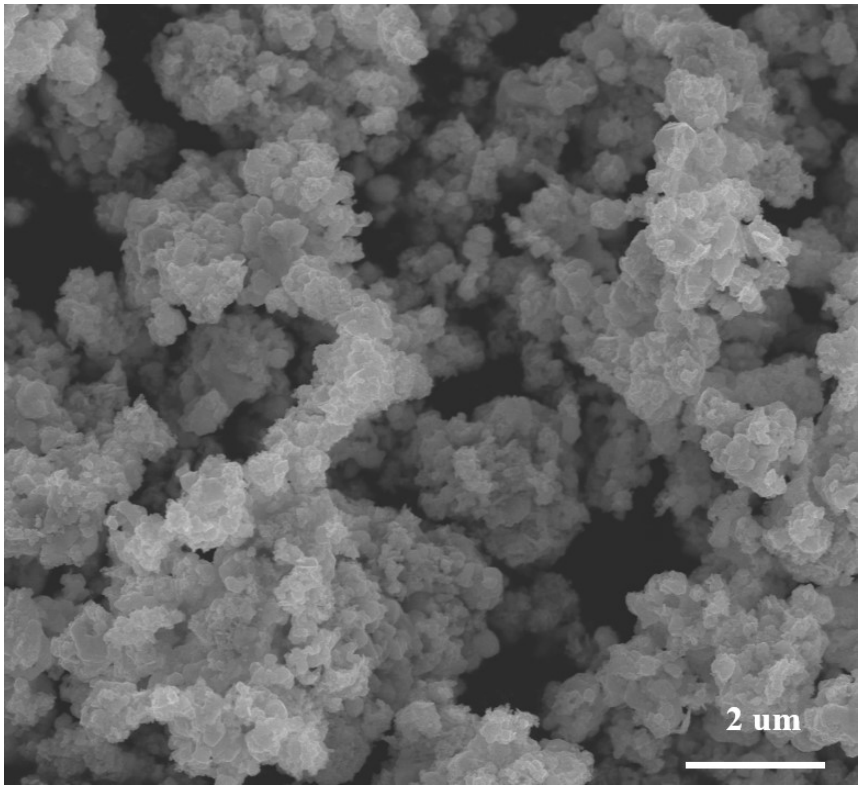

Fig. S3 SEM image of Ag-NP

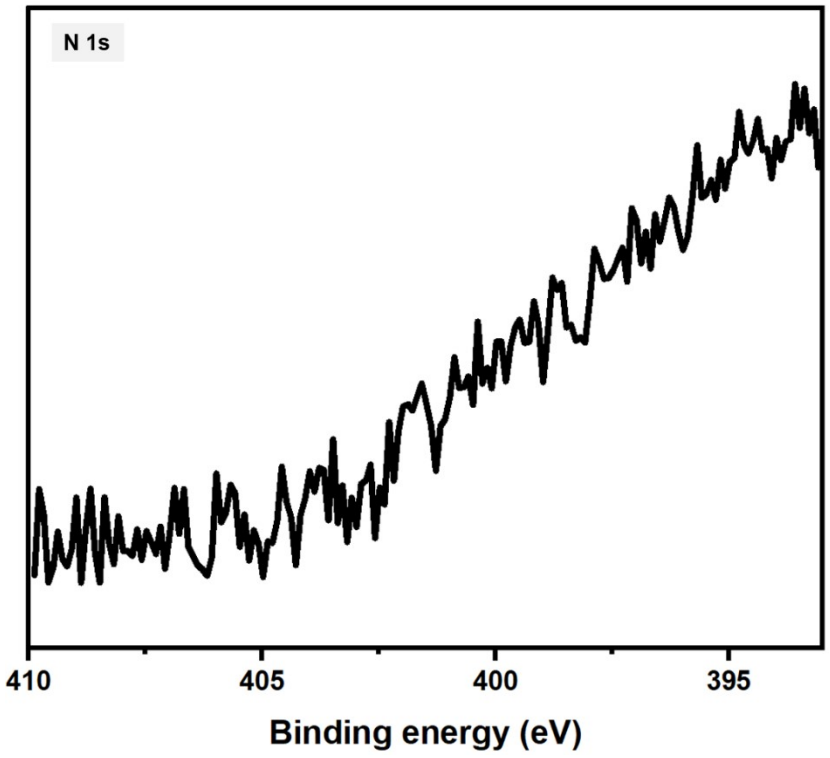

Fig. S4 the N 1s XPS spectrum of Ag-GB

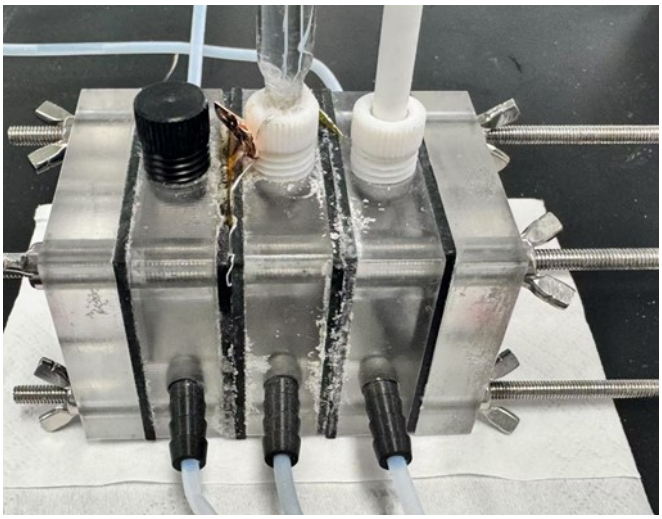

Fig. S5 The image of the customized flow cell

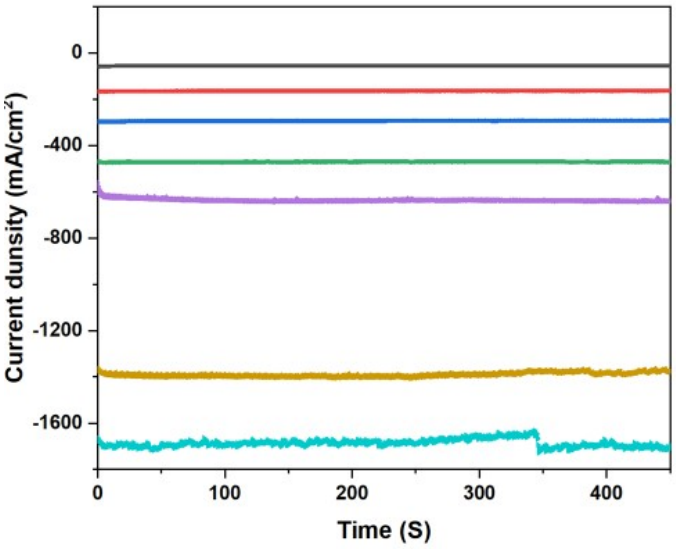

Fig. S6 The representative i-t curves on Ag-GB

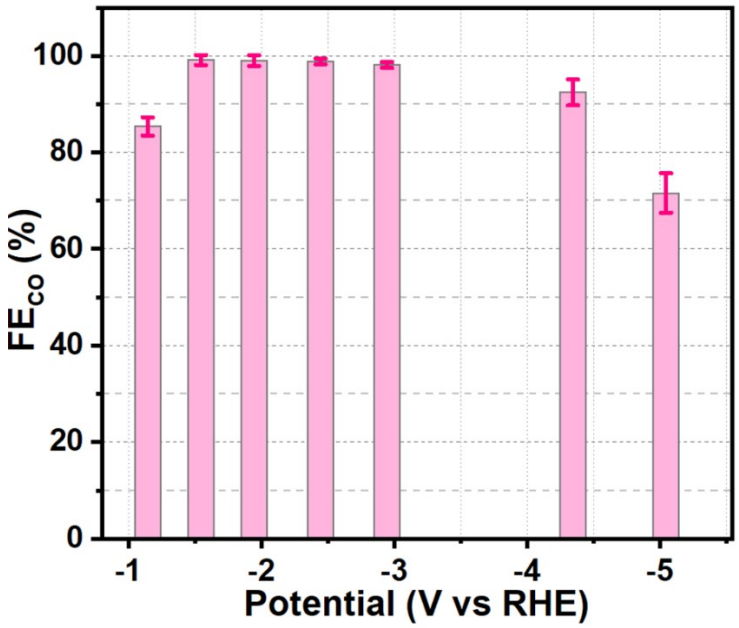

Fig. S7 Potential-dependent FE_{CO} on Ag-GB (without iR correction)

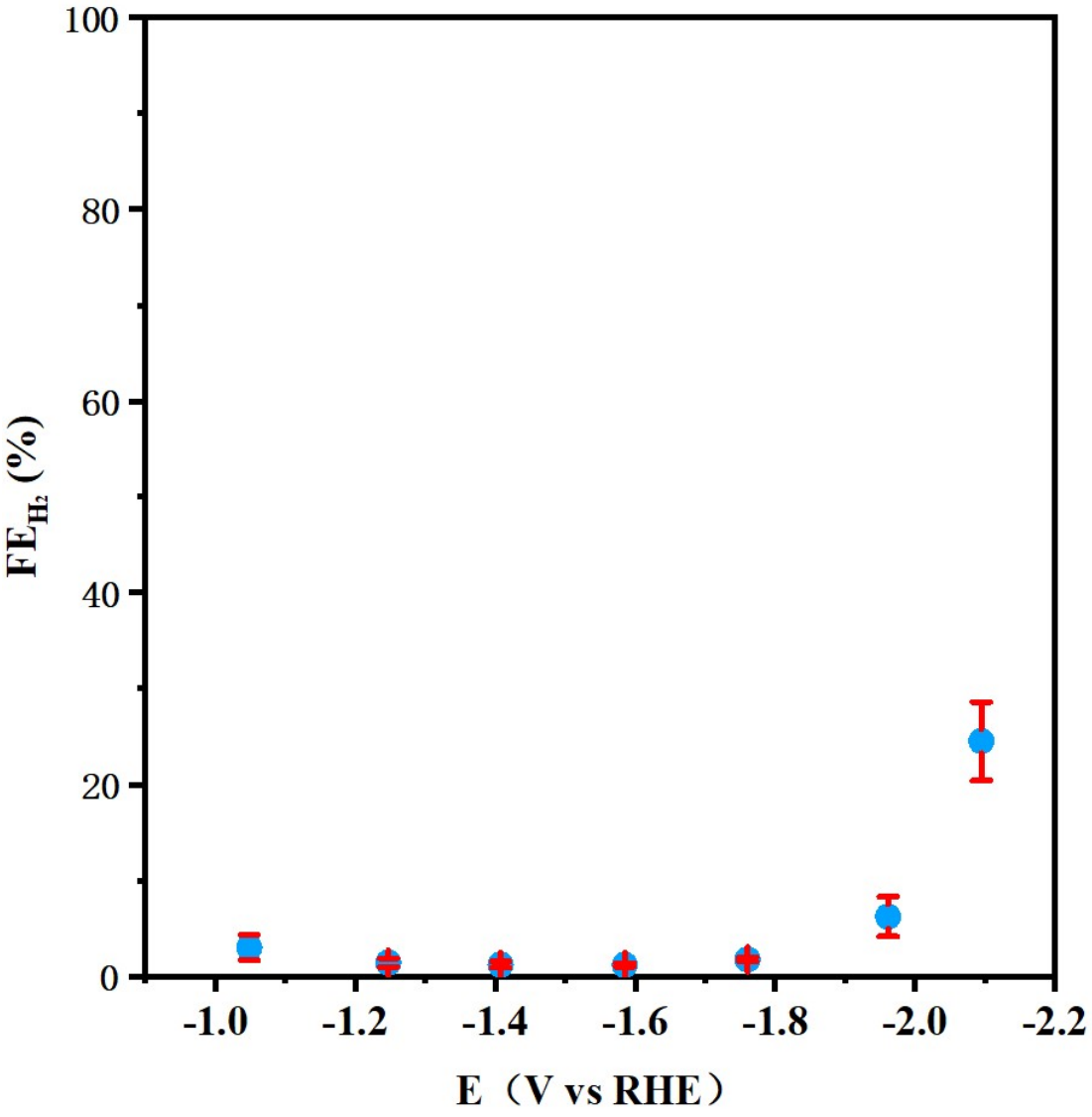

Fig. S8 Potential-dependent FE for H_2 on Ag-GB

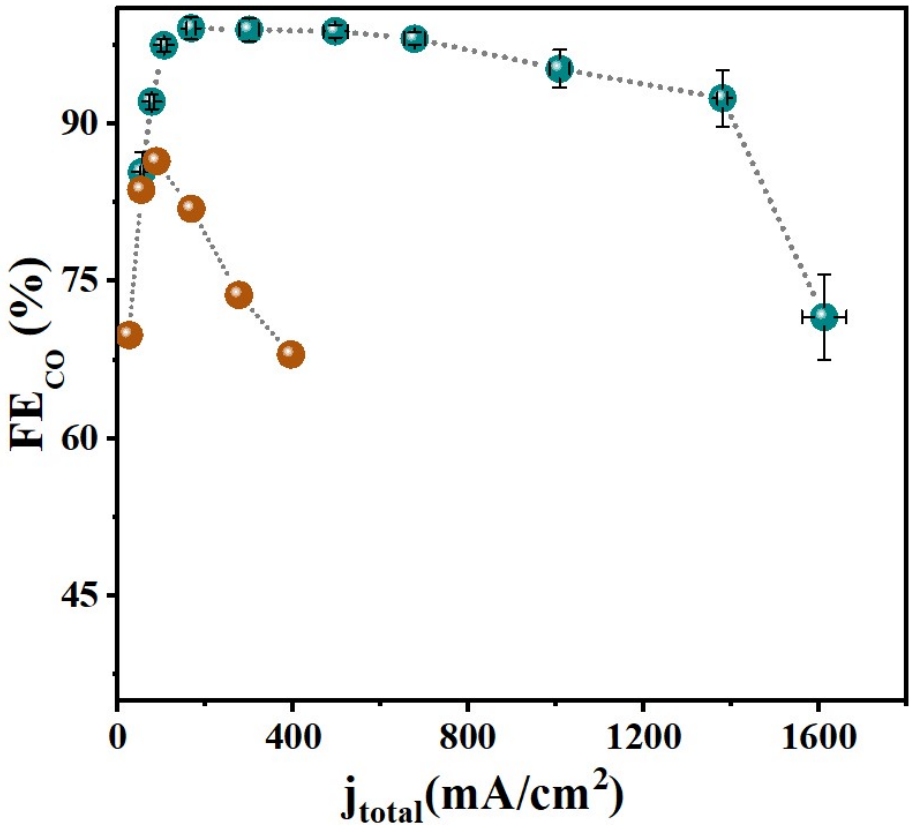

Fig. S9 Current density-dependent FE for CO on Ag-GB

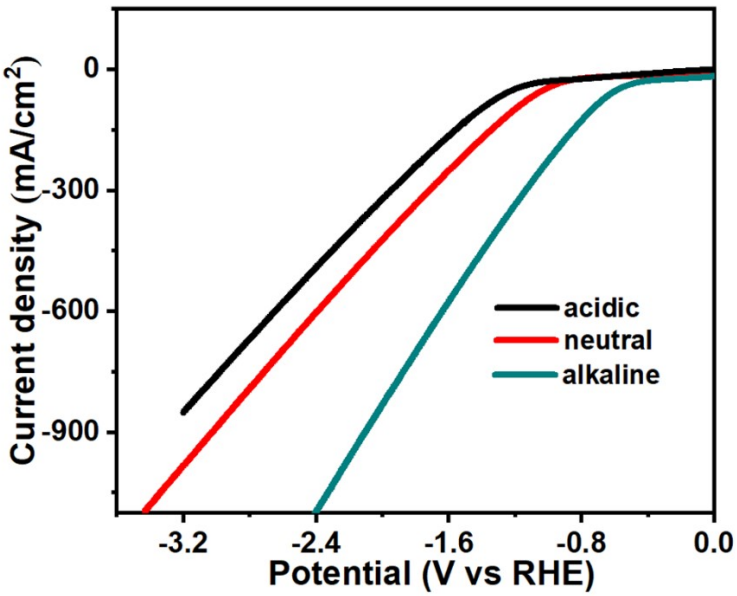

Fig. S10 LSV curves of Ag-GB under CO_2 atmosphere (without iR correction)

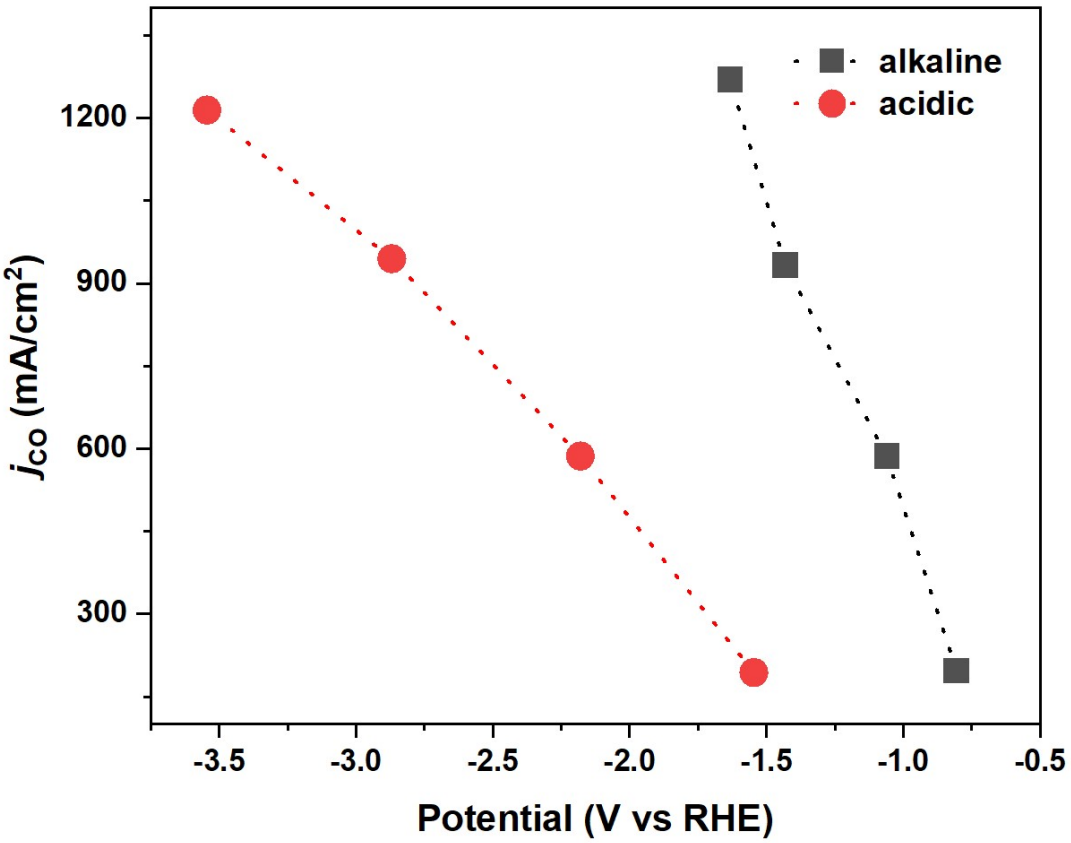

Fig. S11 Potential-dependent j_{CO} on Ag-GB

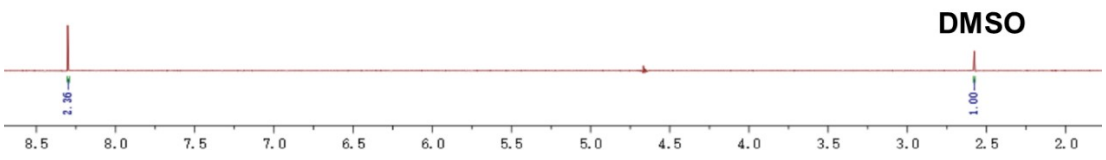

Fig. S12 ^{1}H-NMR of the electrolyte after the stability test. Note: The spectrum was

acquired with water peak suppression.

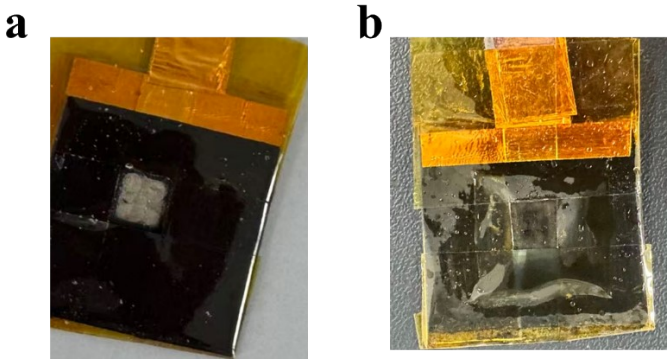

Fig. S13 Photographs of the electrodes after (a) 30 min and (b) 100 h of electrocatalysis.

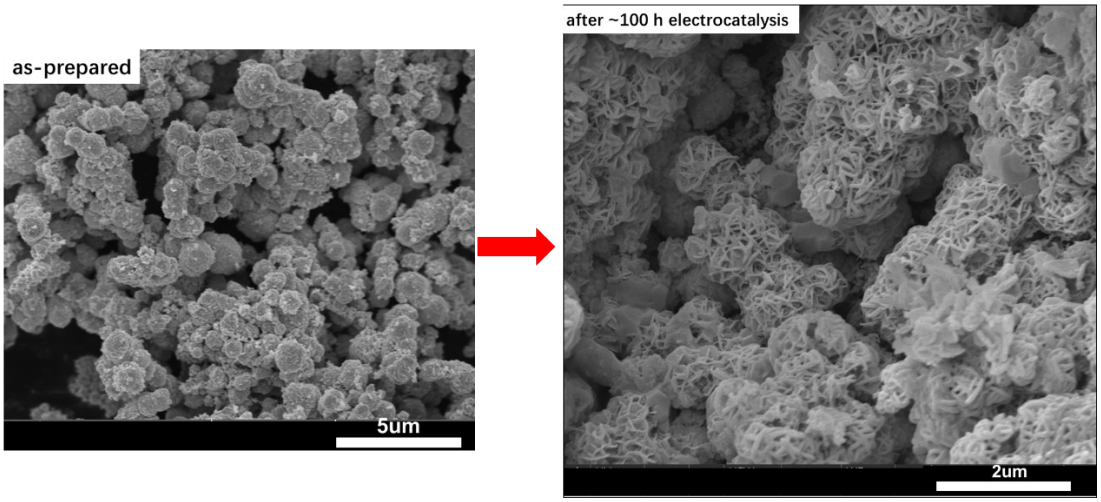

Fig. S14 SEM images of Ag-GB before and after stability test.

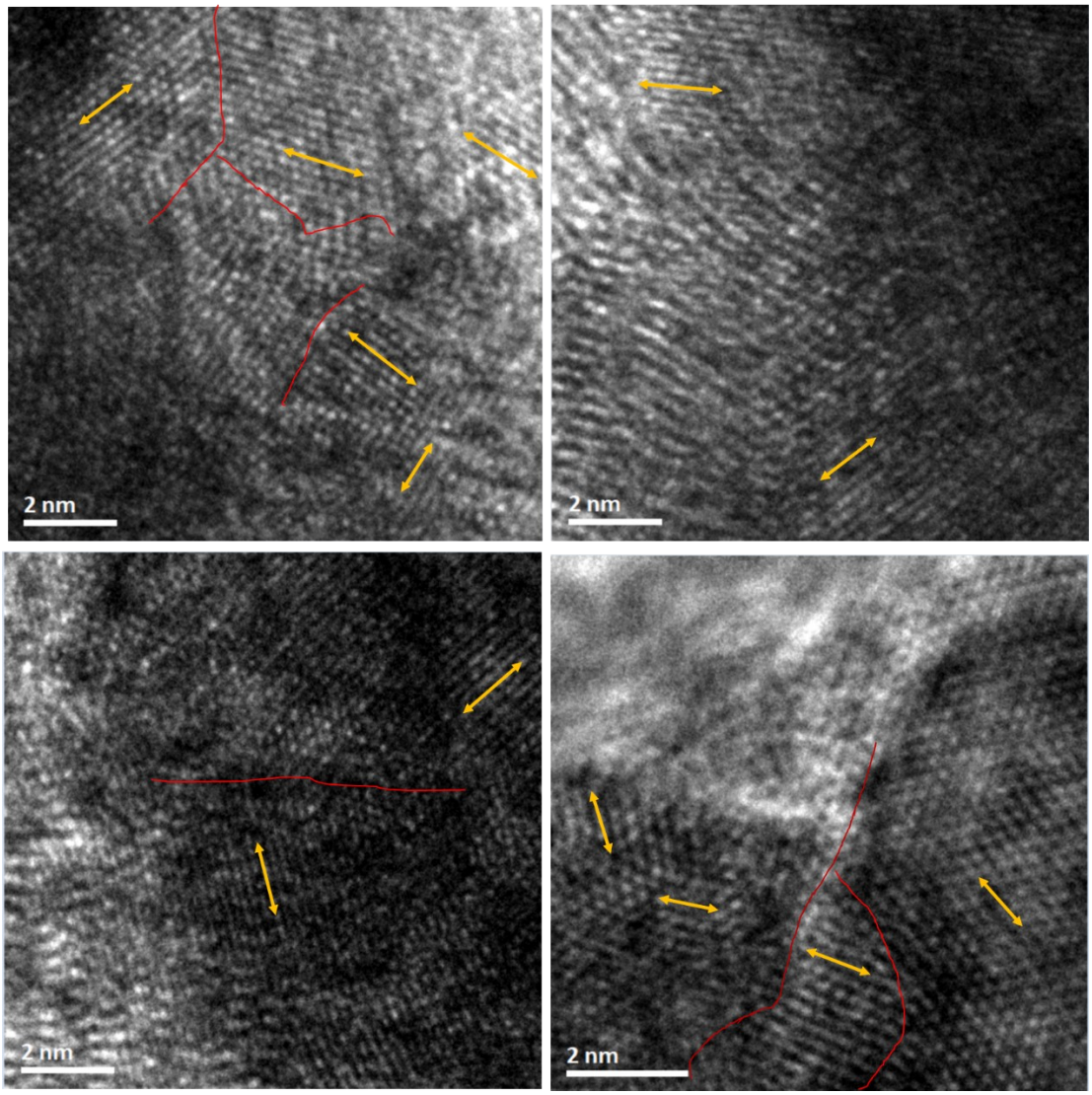

Fig. S15 HR-TEM images of Ag-GB after the stability test.

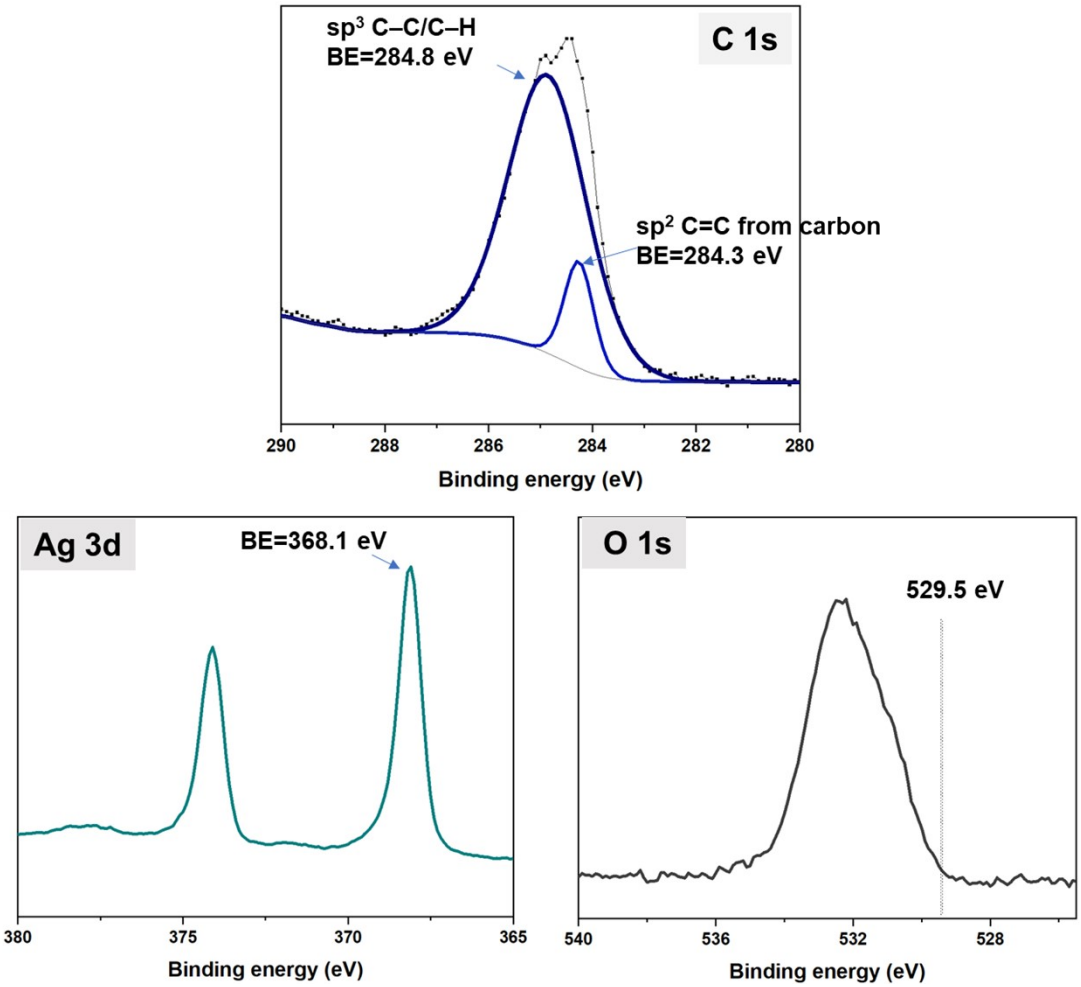

Fig. S16 XPS spectra of Ag-GB after the stability test. Prior to the analysis, the sample was cleaned by Ar^+ ion sputtering to exclude the possible influence of surface oxidation.

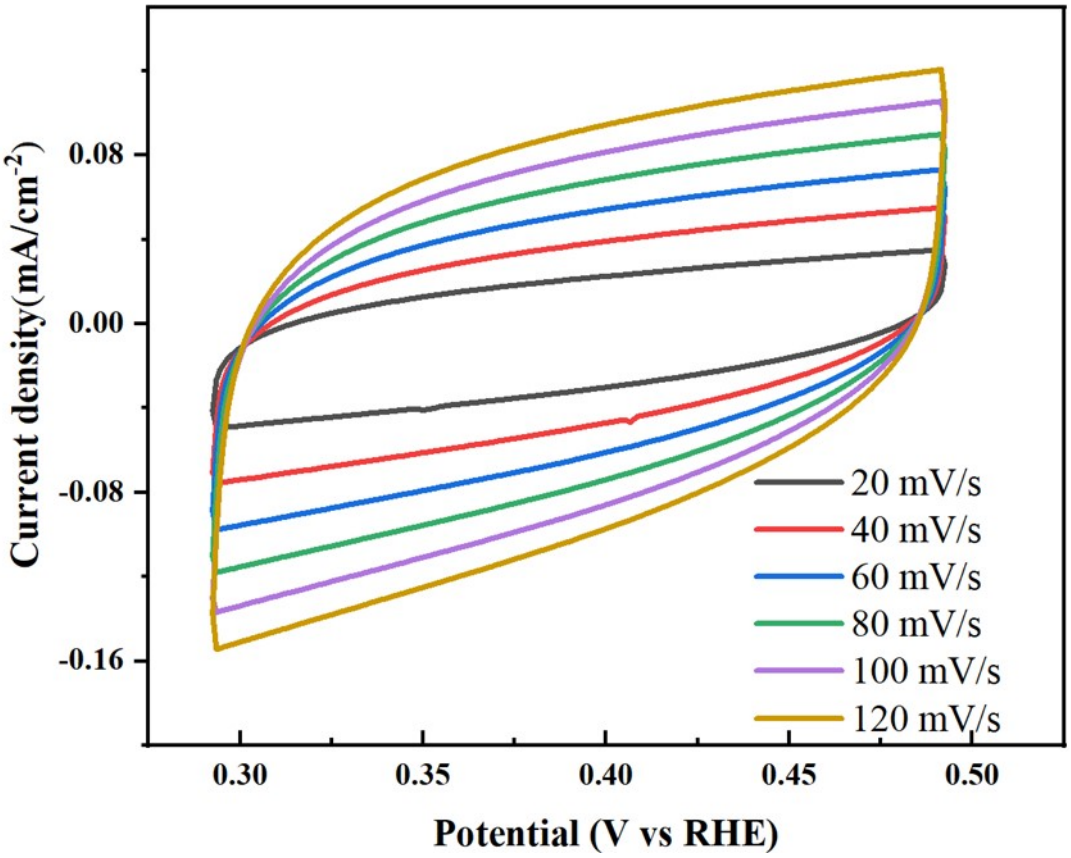

Fig. S17 CV curves of Ag-NP recorded at various scan rates.

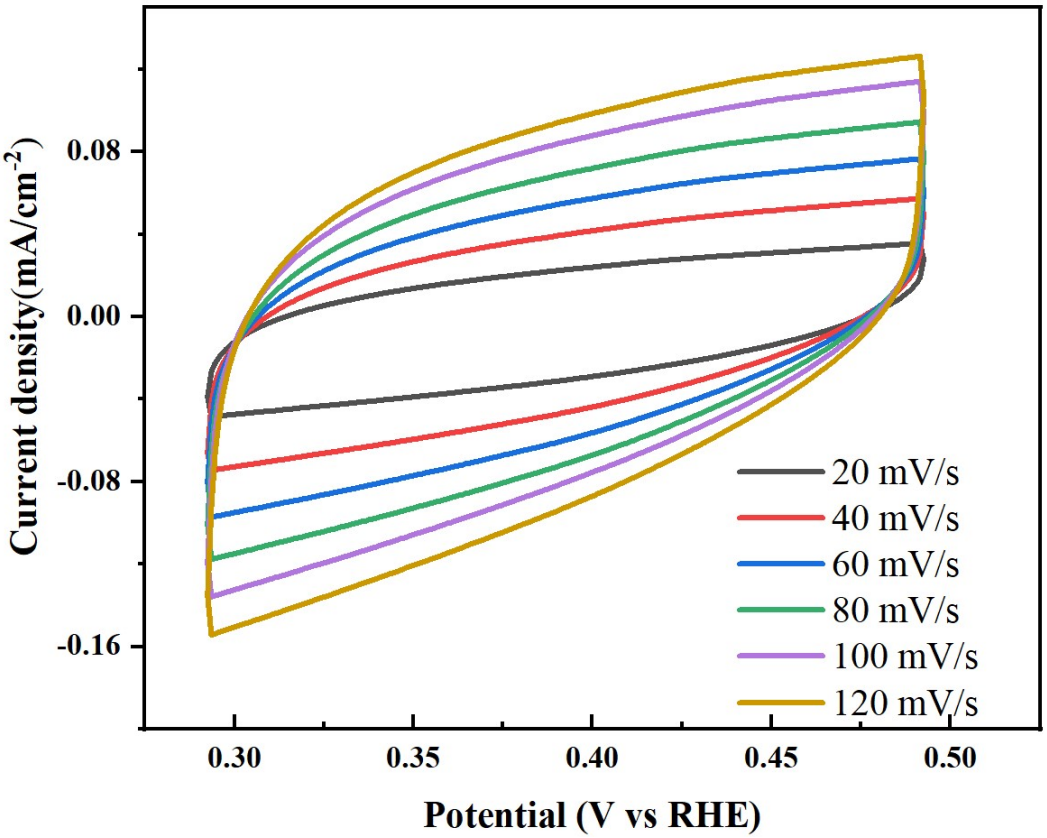

Fig. S18 CV curves of Ag-GB recorded at various scan rates.

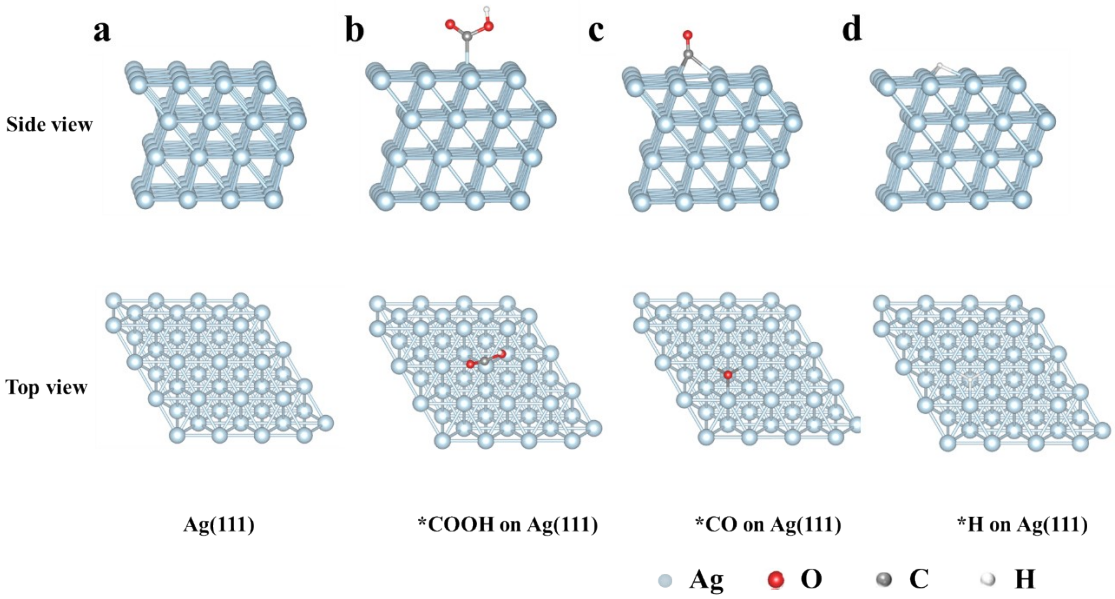

Fig. S19 (a) Representative surface atom configurations of Ag (111). Optimized surface slabs with adsorbed (b) *COOH, (c) *CO and (d) *H on Ag (111) surfaces. The light blue, red, gray and white balls represent Ag, O, C and H, respectively.

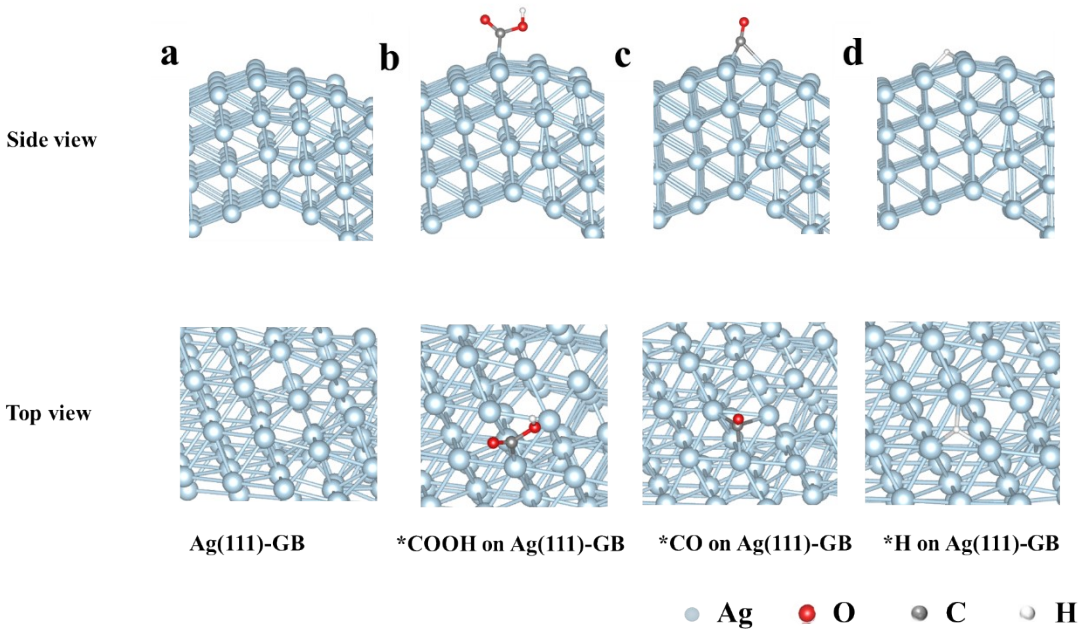

Fig. S20 (a) Representative surface atom configurations of strained Ag (111). Optimized surface slabs with adsorbed (b) *COOH, (c) *CO and (d) *H on Ag (111)-GB surfaces. The light blue, red, gray and white balls represent Ag, O, C and H, respectively.

Table S1. Comparison of recent reported CO_2RR catalysts

Catalyst	Electrolyte	Cell type	Catalyst loading (mg/cm²)	Potential (V vs RHE)	iR correction (%)	j_{CO} (mA/cm²)	FE (%)	Ref.
re-AgS_4	1 M KOH	flow cell	2	<-0.6	N/A[b]	750	93	1
$AuAg_{24}$	0.1 M $KHCO_3$	MEA	1	3.6[a]	0	202.2	90.4	2
Ni–N4/C–NH_2	1 M KOH	flow cell	3	-1	85	447	89	3
Ni@CC-T	1 M KOH	flow cell	1	-1.3	85	399.2	99.8	4
CeO_2/AgNWs	1 M KOH	flow cell	1.5	-1.5	85	251.3	92.1	5
NiNC-PANI	0.1 M $KHCO_3$	MEA	1	~3[a]	0	200	100	6
plasma-treated Ag	0.01 M CsOH	MEA	0.27	3[a]	0	~350	92	7
Ni–N–C-900	1.0 M KOH	flow cell	2	-0.96	N/A[b]	391	98	8
Ni@NiNCM	1.0 M $KHCO_3$	flow cell	1	N/A	N/A[b]	100	>90	9
FNC-SnOF	1.0 M $KHCO_3$	flow cell	1	-0.7	N/A[b]	141	93.8	10
NiPc MDEs	1.0 M $KHCO_3$	flow cell	1	-0.7	100	300	99.5	11
$ClAg_{14}$(C≡CtBu)$_{12}$+ NCs	1 M KOH	MEA	0.28	2.63[a]	0	400	99	12
Sb1Cu	0.5M $KHCO_3$	flow cell	1	-1.16	85	452	90.4	13
ligand-derived Ag	1 M KOH	flow cell	0.3	3.4[a]	0	298.4	>90	14
CuCo-DSAC	1 M KOH	flow cell	1	-0.66	0	500	98.5	15
Ag-GB	0.5 M K_2SO_4	flow cell	0.76	-1.58	80	500	98.8	this work
Ag-GB	0.5 M K_2SO_4	flow cell	0.76	-1.96	80	1282	92.4	this work
Ag-GB	1 M KOH	flow cell	0.76	-0.8	80	198	98.7	this work
Ag-GB	1 M KOH	flow cell	0.76	-1.63	80	1269.2	90.6	this work

Notes: [a]the potential value is related to the full cell volume; [b]the relevant data is not provided in the literature.

Supplementary References

1 J. Chen, X. Liu, S. Xi, T. Zhang, Z. Liu, J. Chen, L. Shen, S. Kawi and L. Wang, *ACS Nano*, 2022, **16**, 13982.

2 S. Yoo, D. Kim, G. Deng, Y. Chen, K. Lee, S. Yoo, X. Liu, Q. Tang, Y. J. Hwang, T. Hyeon and M. S. Bootharaju, *J. Am. Chem. Soc.*, 2025, **147**, 12546.

3 Z. Chen, X. Zhang, W. Liu, M. Jiao, K. Mou, X. Zhang and L. Liu, *Energy Environ. Sci.*, 2021, **14**, 2349.

4 T. Wang, J. Wang, C. Lu, K. Jiang, S. Yang, Z. Ren, J. Zhang, X. Liu, L. Chen, X. Zhuang and J. Fu, *Adv. Mater.*, 2023, **35**, 2205553.

5 Y.-H. Yu, X. Cui, Y.-M. Hong, G.-W. Qin and S. Li, *Appl. Catal., B: Environ.*, 2025, **373**, 125352.

6 S. Brückner, Q. Feng, W. Ju, D. Galliani, A. Testolin, M. Klingenhof, S. Ott and P. Strasser, *Nat. Chem. Eng.*, 2024, **1**, 229.

7 K. Ye, G. Zhang, X.-Y. Ma, C. Deng, X. Huang, C. Yuan, G. Meng, W.-B. Cai and K. Jiang, *Energy Environ. Sci.*, 2022, **15**, 749.

8 Y. Li, N. M. Adli, W. Shan, M. Wang, M. J. Zachman, S. Hwang, H. Tabassum, S. Karakalos, Z. Feng, G. Wang, Y. C. Li and G. Wu, *Energy Environ. Sci.*, 2022, **15**, 2108.

9 X. Wang, X. Sang, C.-L. Dong, S. Yao, L. Shuai, J. Lu, B. Yang, Z. Li, L. Lei, M. Qiu, L. Dai and Y. Hou, *Angew. Chem., Int. Ed.*, 2021, **60**, 11959.

10 W. Ni, Y. Gao, Y. Lin, C. Ma, X. Guo, S. Wang and S. Zhang, *ACS Catal.*, 2021, **11**, 5212.

11 X. Zhang, Y. Wang, M. Gu, M. Wang, Z. Zhang, W. Pan, Z. Jiang, H. Zheng, M. Lucero, H. Wang, G. E. Sterbinsky, Q. Ma, Y.-G. Wang, Z. Feng, J. Li, H. Dai and Y.

Liang, *Nat. Energy*, 2020, **5**, 684.

12 H. Seong, K. Chang, F. Sun, S. Lee, S. M. Han, Y. Kim, C. H. Choi, Q. Tang and D. Lee, *Adv. Sci.*, 2024, **11**, 2306089.

13 J. Li, H. Zeng, X. Dong, Y. Ding, S. Hu, R. Zhang, Y. Dai, P. Cui, Z. Xiao, D. Zhao, L. Zhou, T. Zheng, J. Xiao, J. Zeng and C. Xia, *Nat. Commun.*, 2023, **14**, 340.

14 Y.-J. Ko, C. Lim, J. Jin, M. G. Kim, J. Y. Lee, T.-Y. Seong, K.-Y. Lee, B. K. Min, J.-Y. Choi, T. Noh, G. W. Hwang, W. H. Lee and H.-S. Oh, *Nat. Commun.*, 2024, **15**, 3356.

15 M. Liu, Y. Yang, W. Zhang, G. Wu, Q. Huang, J. Wen and D. Wang, *Angew. Chem., Int. Ed.*, 2025, **64**, e202504423.